Spectroscopy of Hydrothermal Reactions 23: The Effect of OH Substitution on the Rates and Mechanisms of Decarboxylation of Benzoic Acid

Jun Li and Thomas B. Brill*

Department of Chemistry and Biochemistry, University of Delaware, Newark, Delaware 19716

Received: September 9, 2002; In Final Form: January 15, 2003

The decarboxylation rates of aqueous benzoic acid and 12 mono-, di-, and trihydroxy derivatives of benzoic acid were compared by using spectra from a flow reactor FTIR spectroscopy cell operating at 275 bar in the temperature range of 120−330 °C. Each compound was investigated at its natural pH and as the neutral acid (pH = 1.3−1.5). The decarboxylation reactions followed the first-order (or pseudo-first-order) rate law enabling the rate constants and corresponding Arrhenius parameters of the undissociated acids to be obtained. Based on the half-lives of the reactions at 200 °C, the thermal stability of the OH substituted benzoic acids follow the order: 2,4,6 > 2,4 > 2,3,4 > 2,6 > 2,5 > 2,3 > 3,4,5 > 2 > 3,4 > 4. Solutions of 3,5-dihydroxybenzoic and 3-hydroxybenzoic acids and unsubstituted benzoic acid had the highest thermal stability, whereas no decarboxylation was observed up to 330 °C at a residence time of about 45s. In general, the rate order is multiple ortho, para-OH substitution > ortho substitution > para substitution > meta substitution. The range of activation energies for the decarboxylation of OH substituted benzoic acids is 90−97 kJ/mol, and the rate differences are controlled mainly by activation entropy. The transition state structures were determined using density functional theory. Starting from the anti carboxylic hydrogen conformers in the gas phase, the activation energies to the transition state structures having the four-member C−C(O)-O−H ring are 213−260 kJ/mol using B3LYP/6-31G//B3LYP/6-31G and 202−246 kJ/mol using B3LYP/6-31+G(d,p)//B3LYP/6-31G(d). Incorporation of one water molecule forms a six-member cyclic structure, which dramatically reduces the activation energy by about 120−130 kJ/mol using B3LYP/6-31G//B3LYP/6-31G and by about 75 kJ/mol using B3LYP/6-31+G(d,p)//B3LYP/6-31G(d). In the water-catalyzed transition state structure, the water molecule acts as a bridge linked by two hydrogen bonds which enables concerted proton transfer and C−(CO_2H) bond cleavage to occur. Although the calculated activation energy approximately follows the trend of the experimental half-lives, the experimental activation entropy appears to dominate in determining the rates.

Introduction

Reaction chemistry of organic compounds in hydrothermal environments has received much attention because of its importance for understanding the formation of fossil fuels and potential green chemical processes.[1−6] Many classes of organic compounds that are regarded to be unreactive in aqueous solution undergo diverse chemical reactions when the temperature is increased above the boiling temperature of water. Water molecules can participate in the reactions in various ways such as a catalyst, reactant, and solvent,[7] as a result of its dramatic changes in density, dielectric constant, and ionization constant with increasing temperature, as well as its effect on the solubility of the solute.

Aromatic carboxylic acids are among the primary compounds of interest in the formation of fossil fuels and in determining the organic carbon distribution in natural aqueous systems. Detailed information about the reaction rates and pathways of aromatic carboxylic acids at hydrothermal conditions are therefore needed for modeling of these systems. The decarboxylation of benzoic acid and several OH substituted benzoic acids has been studied. Benzoic acid is more stable at hydrothermal conditions than the OH substituted benzoic acids. Katrizky et al.[8] observed that only 0.1% of benzoic acid converted to benzene after 6 h at 350 °C. When a mineral redox buffer[9] or a fairly strong base[8] was present, however, the decarboxylation of benzoic acid was accelerated. Electron-withdrawing substituents, such as OH[10−13] and NO_2,[14] lower the thermal stability of benzoic acid. The decarboxylation rate of OH substituted benzoic acids at hydrothermal conditions is pH dependent. Gallic acid[11] (3,4,5-trihydroxybenzoic acid), a naturally occurring aromatic acid, decarboxylates faster at pH = 7.0 than at pH = 4.3, which means that the anion has a faster decarboxylation rate than the neutral acid. When a strong acid was added to a solution of 2,4-dihydroxybenzoic acid[13] or 2,4,6-trihydroxybenzoic acid,[12] the decarboxylation rate initially increased with increasing acidity and then remained constant. Kinetic hydrogen[15,16] and carbon[17] isotopic effects were used to clarify the reaction mechanism. The rate-determining step changed from slow proton transfer to C−C bond cleavage as the solution was made more acidic. Segura et al.[14] did not observe a significant solvent effect in the decarboxylation rate of dinitrobenzoate anions. Hydrolytic ionic reaction chemistry dominates thermal (free-radical) routes at subcritical hydrothermal conditions. Generally, a carbanion reaction mechanism (S_E1) has been assumed in the decarboxylation of substituted and unsubstituted benzoic acids.[18,19]

Ruelle's theoretical study[18,19] on the decarboxylation of benzoic acid and salicylic acid indicated how water molecules can catalyze the reaction. Because of the low level of theory and computation power at the time, his calculation was restricted and did not agree well with experimental results. A recent

* To whom correspondence should be addressed. brill@udel.edu.

10.1021/jp0220231 CCC: $25.00
Published on Web 03/21/2003

computation study[20] of aromatic nucleophilic substitution of halobenzenes in the gas phase has shown that S_NAr proceeds via a single-step concerted mechanism without the formation of a stable σ complex. Our experimental and computational comparison[21] of decarboxylation of aliphatic dicarboxylic acids showed that decarboxylation proceeds via a concerted proton transfer and C−C cleavage step in the transition state structure in which one water molecule is involved. In the present paper, we extend these studies on the decarboxylation of carboxylic acids beyond aliphatic into aromatic acids. The reactivity and kinetics of decarboxylation of benzoic acid and OH substituted benzoic acids are measured in situ using a flow reactor with FT-IR spectroscopy and are described by density functional theory.

Experimental Section

All acids (benzoic, 2-hydroxybenzoic, 3-hydroxybenzoic, 4-hydroxybenzoic, 2,3-dihydroxybenzoic, 2,4-dihydroxybenzoic, 2,5-dihydroxybenzoic, 2,6-dihydroxybenzoic, 3,4-dihydroxybenzoic, 3,5-dihydroxybenzoic, 2,3,4-trihydroxybenzoic, 2,4,6-trihydroxybenzoic, and 3,4,5-trihydroxybenzoic acids) were purchased from Sigma-Aldrich and used without further purification. Milli-Q deionized water was sparged with compressed Ar before use to expel the atmospheric gases. Solution pH values of aqueous OH substituted benzoic acids and the acidified solutions produced by titration with HCl were recorded with an Orion model 330 pH meter. Because of the relatively low solubility of the acids in pure water, the concentrations of the solutions were 0.025*m*, except for 2-hydroxybenzoic acid (0.01*m*) and 2,3,4-trihydroxybenzoic acid (0.015*m*).

The flow reactor FT-IR spectroscopy cell constructed from titanium with sapphire windows and gold foil seals has been described in detail elsewhere.[22,23] The temperature and pressure were controlled within ±1 °C and ±1 bar, respectively. The chosen flow rate (0.1−1.0 mL/min range) was controlled with an accuracy of 1% by the use of an Isco syringe pump. Correction of the flow rate was made to account for the density change with temperature. Data were collected in the 120−280°C range, although 3-hydroxybenzoic acid, 3,5-hydroxybenzoic acid, and unsubstituted benzoic acid were subjected to temperatures up to 330 °C and found not to react at a residence time of 45 s. Transmission IR spectra were recorded at 4 cm^{-1} resolution with a Nicolet 560 Magna FTIR spectrometer and an MCT-A detector. Background spectra recorded for pure water at the same conditions were subtracted. Thirty-two spectra were summed at each condition and the rate data reported herein are the average of three replicated measurements.

During the decarboxylation reaction, only the asymmetric stretching mode of aqueous CO_2 centered at 2343 cm^{-1} was observed in the band-pass of the sapphire windows. To obtain the kinetic parameters, the band area of CO_2 was converted into concentration at each condition by using the Beer−Lambert Law and the previously determined molar absorptivity of aqueous CO_2.[24] Weighted least-squares regression[25] with a 95% confidence interval was performed in which the statistical weight was set to be $1/\sigma^2$, where σ is the standard deviation of the variables.

An advantage of the use of the small-scale flow reactor is that any precipitation of the reactant or products is readily detected in the form of disruption of the flow rate. The relatively low solubility of benzoic acid and its derivatives in water might result in such an event. However, no irregularity was found in the flow rates in any of the experiments. Decomposition by the loss of −OH is a reaction known to occur at higher temperatures than were used in this work,[26] but it forms an insoluble precipitate that was not found here.

Conformational analyses of the acids and the transition state structures for decarboxylation were performed by density functional theory calculations using Gaussian 98[27] software at the level of B3LYP theory.[28,29] The 6-31G basis set was used for conformation analyses. The ground state and transition state structures were first optimized with the 6-31G basis set and then further optimized with the 6-31G(d) basis set. Vibrational frequency analyses were conducted to confirm that the optimized geometry was a local minimum or a transition state and provided thermal corrections to the thermal energy, enthalpy, and free energy. The effects of temperature and pressure were considered at 200 °C and 275 bar at the level of B3LYP/6-31G(d) theory. Finally, activation energies were calculated based on single-point energy calculations at the level of B3LYP/6-31+G(d,p) theory based on the thermal correction to 200 °C and 275 bar at the level of B3LYP/6-31G(d) with the scaling factor 0.9804. It was found that these temperature and pressure corrections had a negligible effect.

A comparison by Bach et al.[20] has shown that the activation barriers were overestimated at the MP2 level and underestimated at the B3LYP level, but the difference at these levels is small. The results are least accurate at the Hartree−Fock level which was not used here. The absolute value of the barrier is not vital for this paper because the focus is on the relative comparison of the activation energies.

Results and Discussion

Decarboxylation Kinetics. The overall decarboxylation reaction of OH substituted benzoic acids followed eq 1

$$(HO)_nArCO_2H \rightarrow (HO)_nAr + CO_2 \qquad (1)$$

A large difference in the hydrothermal stability exists however as a result of the position of the OH substituents on the benzene ring. For example, 3-hydroxybenzoic and 3,5-dihydroxybenzoic acids did not decarboxylate below 330 °C with a residence time of 45 s, whereas 2,4,6-trihydroxybenzoic acid began to decompose at 50 °C.

Reaction 1 was clearly indicated by in situ FT-IR spectroscopy. As an example, Figure 1 presents FT-IR spectra of the aqueous 2,4-dihydoxybenzoic acid solution (0.025*m*) at different temperatures, 275 bar, and a residence time of 45 s. Unfortunately, no absorbance for aqueous CO_2 was observed for aqueous neutral and basic solutions because of the low solubility of the OH substituted benzoic acids and hydrolysis of CO_2.[30] The hydrolysis of CO_2 in the acidic solutions (either natural or obtained by adding HCl) was calculated to be negligible in this work, even through these benzoic acids are weak.

The rate constants of the undissociated acids were determined in acidified solutions where the predominant species is the neutral acid. The solution pH_{25} values of 1.3 or 1.5 prepared by adding HCl were suitable for real time FT-IR spectroscopy at hydrothermal conditions because 99% of the acid is in the neutral form at 25 °C. The ratio is even higher when extrapolation is made to higher temperatures, because the ionization constant of H_2O increases and dissociation constant of the acids decreases with increasing temperature. The dissociation constants of the acids needed for the charge balance analysis were obtained by extrapolation of the ionization constant[31] and specific volume[32] of water from room temperature[33] to higher temperatures using the iso-Coulombic method.[34] Corrosion and leakage are the two leading factors which limit the use of flow

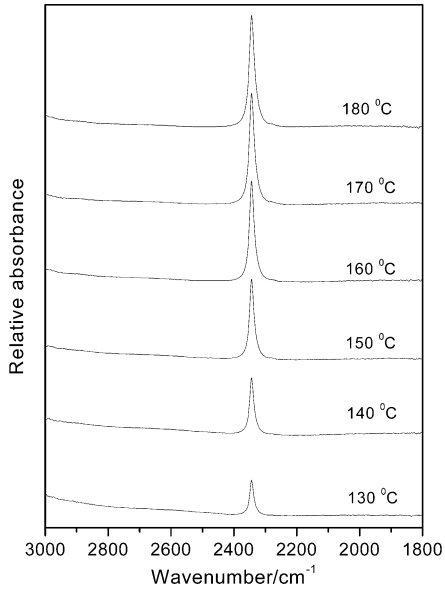

Figure 1. In situ FT-IR spectra of the 0.025*m* 2,4-dihydroxybenzoic acid solution at different temperatures, a pressure of 275 bar, and a residence time of about 45 s.

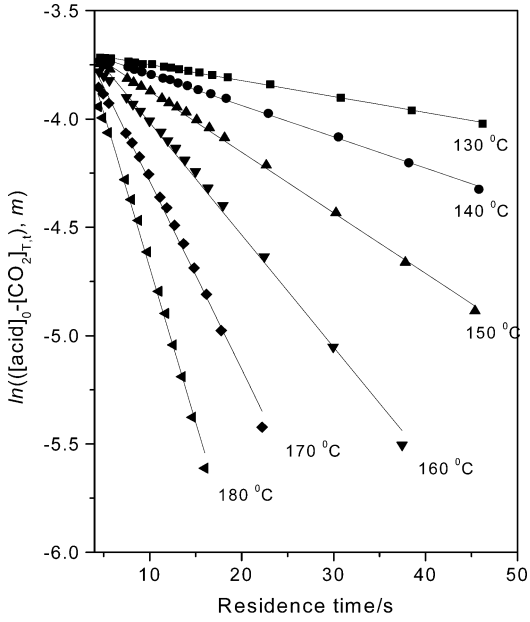

Figure 2. Rate plot for the decarboxylation of the 0.025*m* 2,4-dihydroxybenzoic acid solution at different temperatures.

reactor spectroscopy at even more acidic solutions at high temperature and pressure.

Based on the rate of formation of CO_2, a plot of $\ln([acid]_0-[CO_2]_T)$ vs residence time (Figure 2 is an example) provides the decarboxylation rates, where $[acid]_0$ is the initial concentration of the benzoic acid. At low temperature (low extent of reaction), the rates extrapolate well to the initial concentration. At high temperature, this extrapolation is not accurate for the reason that, at fast flow rate and high temperature, the cell is probably at or beyond the limit of the assumption of uniform temperature.[23] The first-order rate law applied to the data in Figure 2 and the resulting rate constants of OH substituted benzoic acids at their natural pH and more acidic conditions are listed in Table 1. The variation of the rate constants with temperature for the undissociated acids followed the Arrhenius equation. The Arrhenius plots and resulting parameters, as well

TABLE 1: Observed First-Order or Pseudo-First-Order Rate Constants ($k_{obs} \times 10^3$) of Mono-, Di-, and Trihydroxybenzoic Acids at Different Values of the Solution pH

2-hydroxybenzoic acid(0.01*m*)			4-hydroxybenzoic acid(0.025*m*)			2,3-dihydroxybenzoic acid(0.025*m*)		
temp/°C	$pH_{25} = 1.34$	$pH_{25} = 2.68^a$	temp/°C	$pH_{25} = 1.52$	$pH_{25} = 3.23^a$	temp/°C	$pH_{25} = 1.42$	$pH_{25} = 2.50^a$
210		7.09±0.19	210		1.42±0.08	190		6.498±0.21
220	9.67±0.19	10.61±0.37	220	3.67±0.08	2.44±0.09	200	7.46±0.33	10.97±0.27
230	15.82±0.30	17.75±0.59	230	5.19±0.20	3.68±0.08	210	12.39±0.22	17.74±0.38
240	27.93±0.45	27.35±0.51	240	8.41±0.21	5.91±0.17	220	20.20±0.33	26.95±0.49
250	38.89±1.23	40.11±0.74	250	12.81±0.31	8.15±0.30	230	35.48±0.86	40.01±0.90
260	52.91±0.88		260	19.21±0.50		240	52.35±1.23	
270	77.23±3.04		270	28.21±0.68		250	75.56±1.68	

2,4-dihydroxybenzoic acid(0.025*m*)			2,5-dihydroxybenzoic acid(0.025*m*)			2,6-dihydroxybenzoic acid(0.025*m*)		
temp/°C	$pH_{25} = 1.32$	$pH_{25} = 2.57^a$	temp/°C	$pH_{25} = 1.35$	$pH_{25} = 2.52^a$	temp/°C	$pH_{25} = 1.40$	$pH_{25} = 2.04^a$
130	10.99±0.26	7.36±0.08	190	4.60±0.19		120	2.62±0.04	
140	22.63±0.37	14.45±0.16	200	7.67±0.14		130	6.13±0.13	3.26±0.05
150	47.69±1.21	27.98±0.31	210	13.82±0.38	8.5±0.11	140	12.86±0.15	6.60±0.11
160	77.53±1.60	54.75±1.11	220	20.70±0.37	13.83±0.17	150	21.99±0.19	13.74±0.17
170	141.91±5.70	86.79±1.81	230		22.39±0.61	160	38.28±0.39	26.19±0.37
180	223.2±10.5	148.3±3.8	240		37.86±1.49	170	66.26±0.65	51.09±0.77
			250		51.57±1.92	180		86.73±2.55

3,4- dihydroxybenzoic acid(0.025*m*)			3,4,5-triihydroxybenzoic acid(0.025*m*)			2,3,4-triihydroxybenzoic acid(0.015*m*)		
temp/°C	$pH_{25} = 1.45$	$pH_{25} = 3.13^a$	temp/°C	$pH_{25} = 1.51$	$pH_{25} = 3.11^a$	temp/°C	$pH_{25} = 1.36$	$pH_{25} = 2.68^a$
210		3.76±0.22	200		3.24±0.22	130	8.12±0.06	
220	6.16±0.11	5.29±0.20	210		5.51±0.22	140	16.17±0.17	
230	10.02±0.28	8.6±0.21	220		9.40±0.21	150	30.67±0.19	20.24±0.26
240	17.51±0.50	13.65±0.21	230	17.23±0.52	14.97±0.19	160	55.91±0.71	36.14±0.40
250	22.43±0.49	20.29±0.52	240	30.06±1.01	23.48±0.55	170	94.82±1.95	61.39±0.63
260	38.22±1.85		250	44.68±1.24	36.05±0.65	180	133.6±2.9	101.9±2.0
			260	62.06±1.30		190		160.9±4.9
			270	93.74±2.49		200		240.4±8.2
			280	145.5±4.3				

[a] Natural solution pH.

TABLE 2: Experimentally Determined Arrhenius Parameters and Calculated Activation Parameters with and without H_2O Incorporation for OH Substituted and Unsubstituted Benzoic Acids

	experimental				calc E_a/kJ mol^{-1}				
					B3LYP/6-31G//B3LYP/6-31G[b]		B3LYP/6-31+G(d,p)//B3LYP/6-31G(d)[c]		
acid	E_a/kJ mol^{-1}	ln(A,s^{-1})	$\Delta S^{\ddagger}$/J K^{-1} mol^{-1} 200 °C	$t_{1/2}$/s 200 °C	without H_2O	with H_2O	without H_2O	with H_2O	$\Delta S^{\ddagger}$/J K^{-1} mol^{-1} 200 °C [d]
benzoic acid					259.18	131.97	245.94	175.24	−105.80
2-hydroxybenzoic acid	92.04±5.32	17.88±1.26	−108.41	172.34	225.26	95.56	217.89	138.71	−108.20
3-hydroxybenzoic acid					260.32	133.74	247.79	176.38	−104.35
4-hydroxybenzoic acid	91.54±1.50	16.70±0.34	−118.22	493.93	247.46	117.49	234.11	158.40	−110.33
2,3-dihydroxybenzoic acid	96.69±2.58	19.70±0.63	−93.27	91.06	227.23	102.93	219.57	144.78	−106.66
2,4-dihydroxybenzoic acid	93.20±2.83	23.34±0.81	−63.01	0.98	213.50	89.34	204.99	128.44	−108.22
2,5-dihydroxybenzoic acid	96.13±3.95	19.58±0.98	−94.27	88.86	230.36	104.76	221.19	146.08	−106.53
2,6-dihydroxybenzoic acid	92.12±3.16	22.07±0.89	−73.57	2.66	228.86	98.93	212.60	130.49	−102.82
3,4-dihydroxybenzoic acid	95.86±5.40	18.31±1.28	−104.83	296.04	246.66	118.29	234.92	159.89	−110.05
3,5-dihydroxybenzoic acid					259.02	131.46	246.31	174.01	−106.07
3,4,5-trihydroxybenzoic acid	93.20±.99	18.27±0.92	−105.16	156.70	243.05	115.06	231.97	156.45	−110.72
2,3,4-trihydroxybenzoic acid	89.87±2.33	22.04±0.68	−73.82	1.55	217.87	94.05	208.94	133.09	−107.03
2,4,6-trihydroxybenzoic acid	82.01[a]	24.31[a]	−54.95	0.02	219.93	89.02	202.20	118.12	−107.14

[a] From Schubert, W. M.; Gardner, J. D. *J. Am. Chem. Soc.* **1953**, *75*, 1401. [b] At 25 °C and 1 bar. [c] At 200 °C and 275 bar. [d] Incorporating one water molecule at the level of B3LYP/6-31G(d) theory.

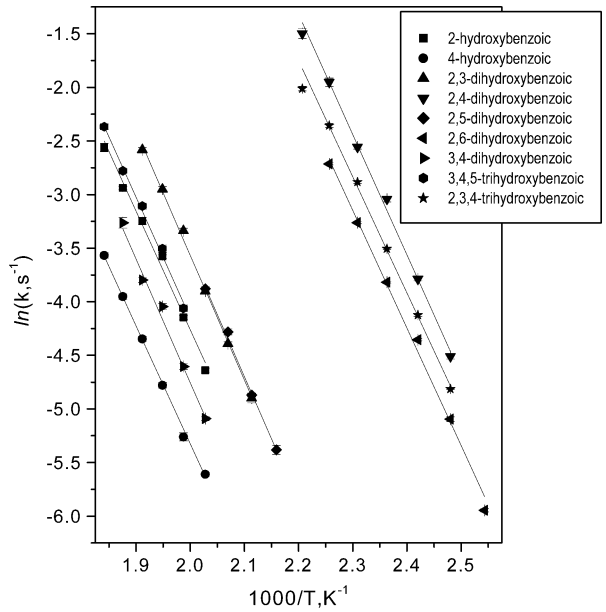

Figure 3. Arrhenius plot for the decarboxylation of OH substituted undissociated benzoic acids.

as half-lives of the decarboxylation reactions, are shown in Figure 3 and Table 2, respectively. The following conclusions were drawn from these data: (1) the effect of a single OH substitutent on the decarboxylation rate follows the order: o- > p > m-; (2) when a second OH substituent exists, if the first substitution occurs at the ortho position, the decarboxylation rate order is: o-,p- > o-,o > o-,m-; if the first OH substituent is at the meta position, the order is the same as in (1), i.e., m-,o > m-,p- > m-,m-; (3) for three OH substituents, substitution at the ortho and para positions causes the fastest decarboxylation rate; (4) meta substitution (both single and double) has only a very small effect on the decarboxylation rate and leads to stability comparable to that of benzoic acid.

The activation energies of OH substituted benzoic acids fall into a narrow range of 90−97 kJ/mol with an average of 93.5 kJ/mol, which resembles the previously reported value for gallic acid of 116 kJ/mol at pH = 4.3,[11] but are smaller than those of NO_2 substituted benzoic acids.[14] The larger activation energy of *o*-NO_2 substituted benzoic acids, for example, can be explained by the larger steric effect of the NO_2 group and stronger hydrogen bonding between the CO_2H group and NO_2 group compared to an OH substituent. The similarity of the activation energies for OH substituted benzoic acids suggests that decarboxylation proceeds via an analogous transition state structure in all cases. The difference in the decarboxylation rates originates primarily from the contribution of the activation entropy.

The effectiveness of *o*- and *p*-OH substitution in promoting decarboxylation can be explained by the resonance contribution. The OH substituent is electron-withdrawing. The developing negative charge on the ipso carbon atom in the transition state can be transferred to the ortho or para position via the resonance effect, thereby stabilizing the transition state structure. The resonance effect is indicated by the following transition state structure calculations using density functional theory.

Geometries and Energetics. The conformational analyses in gas phase of benzoic acid and OH substituted benzoic acids were performed at the level of B3LYP/6-31G theory. The number of conformers found for each of the following acids is given parenthetically: benzoic (2), 2-hydroxybenzoic (7), 3-hydroxybenzoic (8), 4-hydroxybenzoic (4), 2,3-dihydroxybenzoic (11), 2,4-dihydroxybenzoic (14), 2,5-dihydroxybenzoic (14), 2,6-dihydroxybenzoic (6), 3,4-dihydroxybenzoic (12), 3,5-dihydroxybenzoic (8), 2,3,4-trihydroxybenzoic (16), 2,4,6-trihydroxybenzoic (6), and 3,4,5-trihydroxybenzoic acids (10). (Details can be found in Table S, in the Supporting Information). Nagy et al.[35,36] found 2, 8, and 4 conformers for benzoic, 2-hydroxybenzoic, and 4-hydroxybenzoic acid, respectively. Using density functional theory, we found that one of their eight conformers for 2-hydroxybenzoic acid (structure 1), in which all of the atoms lie in one plane, is not a stationary conformer but is a second-order saddle point on the potential energy surface. Shapley et al.[37] compared the hydrogen bonding and solvation energies of *o*-, *m*-, and *p*-hydroxybenzoic acids.

From our conformational analyses, we have drawn the following conclusions: (1) The anti carboxylic conformers are energetically higher than the syn carboxylic conformers. (2) Anti carboxylic conformers have a nonplanar arrangement of −OH groups except when the substitution occurs at single ortho position. The intramolecular hydrogen bonding between the carboxylate group and one ortho hydroxyl group leads to a planar conformation for mono ortho OH substituted benzoic acids. The carboxylate group shares the same plane as the

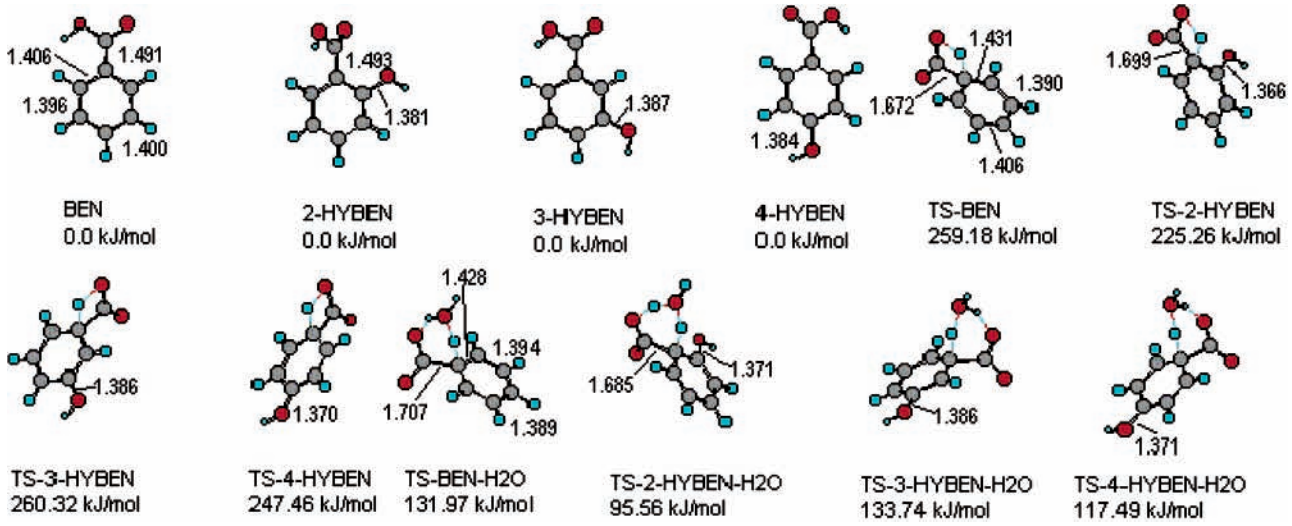

Figure 4. Transition state structures of benzoic acid and monohydroxybenzoic acids with and without one water molecule (B3LYP/6-31G//B3LYP/6-31G). Bond distances are given in angstroms.

benzene ring when two OH groups are placed at the ortho positions (2,6-dihydroxybenzoic and 2,4,6-trihydroxybenzioc acids) at the level of B3LYP/6-31G theory; however, this conformation was a first-order saddle point at the B3LYP/6-31G(d) level. (3) The anti carboxylic conformations with the dihedral angles of 90° and 0° between the carboxylate group and benzene ring are transition state structures for the rotation of carboxylate group. The potential energies at 0° are even lower than those of the stationary conformers. (4) The differences in the potential energies for the anti carboxylic conformations with dihedral angles of the carboxylate group and benzene ring of 0−90° are small at the level of B3LYP/6-31G theory, which means that the rotary energy barriers for the anti carboxylate group are small. (5) Two of the conformers for 3,4,5-trihydroxybenzoic acid have structures 2 and 3 because of the steric effect of the OH groups on the ring. (6) The carboxylate group and the benzene ring of the syn conformer of 2,6-dihydroxybenzoic acid are not coplanar, as is shown by structure 4.

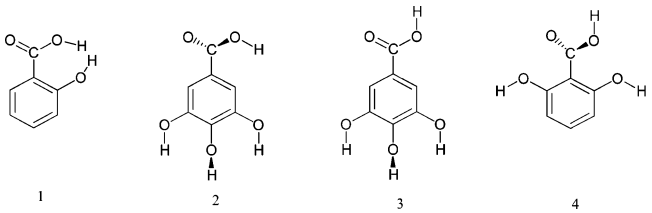

Transition State Structures. Transition state structures for benzoic acid and OH substituted benzoic acids calculated at the level of B3LYP/6-31G theory with and without incorporation of one water molecule are shown in Figures 4−6. The starting structures are anti carboxylic conformers in all cases, but the anti carboxylic conformers for 2,6-dihydroxybenzoic and 2,4,6-trihydroxybenzoic acids are nonplanar at the level of B3LYP/6-31G(d). The calculated activation energies are very high in the gas phase but less than those where the proton acceptor is a β−C−C single bond or a β−C═C double bond.[21] The capability of benzene ring to act as a proton acceptor during the decarboxylation process is comparable to a C≡C triple bond at the β position.[21] In the transition state structures of benzoic acid and OH substituted benzoic acids, the developing negative charge on the ipso carbon atom was dispersed throughout the benzene ring. OH substitution at the ortho or para positions results in more effective charge dispersion and makes the C−OH bond shortens by 0.01−0.02 Å, whereas OH substitution on the meta position has no effect. When one water molecule is involved in the formation of the transition state structure, the activation energies are reduced by about 120−130 kJ/mol with B3LYP/6-31G//B3LYP/6-31G or by about 75 kJ/mol with B3LYP/6-31+G(d,p)//B3LYP/6-31G(d) compared to the free acid, and a six-member cyclic structure results, which is common for the decarboxylation of aliphatic and aromatic carboxylic acids. Incorporation of two water molecules thus forming an eight-member cyclic structure or three water molecules forming ten-member cyclic structure is possible, but involvement of more than one water molecule in the transition state structure is not as effective in reducing the activation barrier toward decarboxylation as is the initial water molecule.[38,39] The effect of the basis set on the activation barriers is different for the transition state structures with and without inclusion of a water molecule. The larger basis set decreases the activation barrier of the transition state structure by about 10 kJ/mol when no water molecule is present and increases it by about 40 kJ/mol with inclusion of the water molecule. The exceptions are 2,6-dihydroxybenzoic and 2,4,6-trihydroxybenzoic acids where the ground state conformation depends on the basis set used. The calculated activation entropies at 200 °C and 275 bar using the B3LYP/6-31G(d) level are relatively similar (about −107 J K^{-1} mol^{-1}). Therefore, by computation of the structures in the gas phase, the activation barrier, rather than the activation entropy, appears to be mainly responsible for the difference in the rate constants.

The experimental data were measured in aqueous solution where a complex solvent field is present. In contrast to the gas-phase DFT model, the experimental E_a values are relatively similar, whereas the differences in activation entropy appear to play the major role in the rate differences (Table 2). It is difficult to identify a specific reason for why the activation entropy is so important, but the most obvious factor appears to be solvation differences of the reactants and transition states. The calculated dipole moments for benzoic acid and the OH substituted benzoic acids are in the order: anti carboxylic conformer reactant < transition state structure with one water molecule < transition state structure without one water molecule. It seems that the transition state structures are more solvated than the reactants and so the high polarity of the water solvent would accelerate the decarboxylation reaction. In contrast to the ground state of the reactants, preferential solvation or desolvation of the

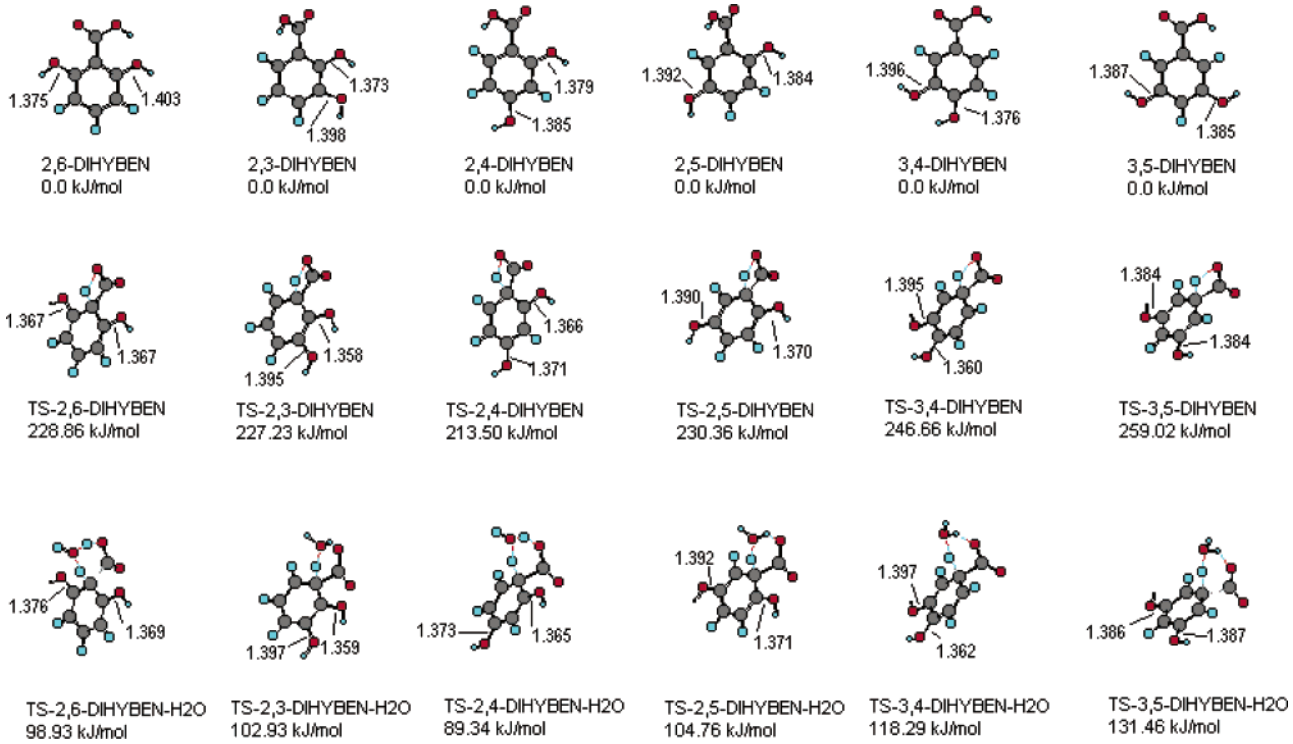

Figure 5. Transition state structures of dihydroxybenzoic acids with and without one water molecule (B3LYP/6-31G//B3LYP/6-31G). Bond distances are given in angstroms.

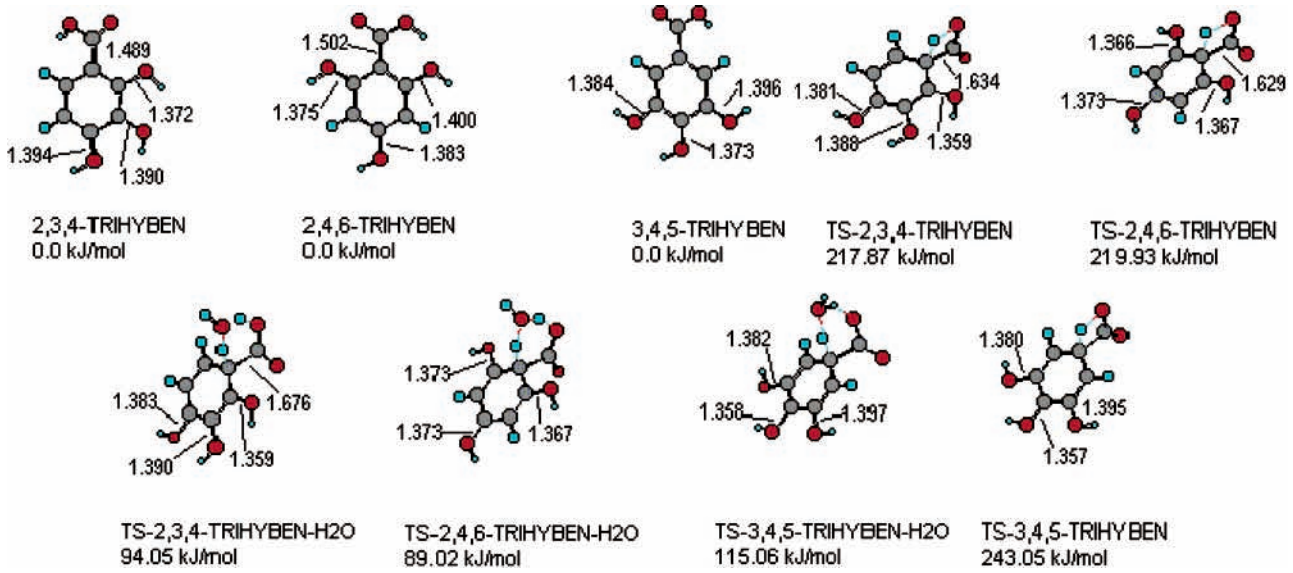

Figure 6. Transition state structures of trihydroxybenzoic acids with and without one water molecule (B3LYP/6-31G//B3LYP/6-31G). Bond distances are given in angstroms.

transition state could reduce or increase the activation energy. An example where preferential solvation reduces the activation energy is the decarboxylation of carbonic acid.[38] An example where the activation energy is increased by desolvation is the decarboxylation of benzisoxazole-3-carboxylic acid.[40,41] Gao[41] reported that the primary contribution of desolvation comes from the difference in the intrinsic charge distribution (i.e., dipole) for the reactant and transition state. When there is no preferential solvation or desolvation in the transition state, the calculated activation energy agrees very well with the experimental result. Another example of this occurrence is the decarboxylation of undissociated acetylenedicarboxylic acid.[21] Unfortunately, solvation differences are probably complex and very difficult to calculate for these hydroxybenzoic acids because (1) there are a number of conformers of the acids and the variety of ways in which H_2O is able to interact with the benzene ring[42] and hydroxyl groups and (2) none of implicit solvation models or the hybrid discrete-continuum model could exactly describe the effect of solvation at present time.[43]

It is interesting to note that the calculated activation energies follow the trend of the experimental half-lives for decarboxylation of the OH substituted benzoic acids. Benzoic acid and the OH substituted benzoic acids having the highest activation energies did not decarboxylate in the present study. The 2,4,6-trihydroxybenzoic acid has the lowest activation energy and decarboxylates easily. It can be seen that the OH substituent effect on the decarboxylation rate is more precisely reflected in the calculated activation energies in the gas phase than in

the experimental results. By comparing the experimental and calculated activation parameters, there is evidence that the decarboxylation rate changes from control by the activation energy in gas phase to control by the activation entropy in aqueous solution.

Conclusions

The experimental decarboxylation rates of hydroxybenzoic acids in solution essentially follow the trend anticipated for conventional aromatic ring resonance effects. The Arrhenius parameters suggest however that the activation entropy as manifested in the preexponential factor is more important in determining the relative rates than is the activation energy. Density functional theory supports that at least one H_2O molecule acts as a bridge and participates in the proton-transfer step of the decarboxylation reaction and that the *trend* in the calculated activation energies qualitatively matches the experimentally found half-lives. However, an apparently more important role in the experimental data is played by the activation entropy. It might be hypothesized therefore that differences in the solvation shell of the reactant and the transition state structures are responsible.

Acknowledgment. We are grateful to the National Science Foundation for support of this work on Grant CHE-9807370.

Supporting Information Available: The **Z** matrixes for the optimized geometries of all benzoic acid derivatives studied in the work using B3LYP/6-31G (Gaussian 98) are compiled in Table S (41 pages). This material is available free of charge via the Internet at http://pubs.acs.org.

References and Notes

(1) Siskin, M.; Katritzky, A. R. *Chem. Rev.* **2001**, *101*, 825.
(2) Katritzky, A. R.; Nichols, D. A.; Siskin, M.; Murugan, R.; Balasubramanian, M. *Chem. Rev.* **2001**, *101*, 837.
(3) Savage, P. A. *Chem. Rev.* **1999**, *99*, 603.
(4) An, J. Y.; Bagnell, L.; Cablewski, T.; Strauss, C. R.; Traino, R. W. *J. Org. Chem.* **1997**, *62*, 2505.
(5) Katrizky, A. R.; Allin, S. A.; Siskin, M. *Acc. Chem. Res*. **1996**, *29*, 399.
(6) Li, C. J.; Chan, T. H. *Organic Reactions in Aqueous Media*; Wiley: New York, 1997.
(7) Akiya, N.; Savage, P. E. *Chem. Rev.* **2002**, *102*, 2725.
(8) Katritzky, A. R.; Balasubramanian, M.; Siskin, M. *Energy Fuel* **1990**, *4*, 499.
(9) Manion, J. A.; McMillen, D. F.; Malhotra, R. *Energy Fuel* **1996**, *10*, 776.
(10) McCollom, T. M.; Seewald, J. S.; Simoneit, B. R. T. *Geochim. Cosmochim. Acta* **2001**, *65*, 455.
(11) Boles, J. S.; Crerar, D. A.; Grissom, G.; Key, T. C. *Geochim. Cosmochim. Acta* **1988**, *52*, 341.
(12) Shubert, W. M.; Gardner, J. D. *J. Am. Chem. Soc.* **1953**, *75*, 1401.
(13) Willi, A. V.; Cho, M. H.; Won, C. M. *Helv. Chim. Acta* **1970**, *53*, 663
(14) Segura, P.; Bunnett, J. F.; Villanova, L. *J. Org. Chem.* **1985**, *50*, 1041.
(15) Willi, A. V.; Cho, M. H.; Chen, W. *Z. Phys. Chem*. **1974**, *91*, 193.
(16) Willi, A. V. *Z. Naturfrorsch*. **1958**, *13A*, 997.
(17) Lynn, K. R.; Bourns, A. N. *Chem. Ind.* **1963**, *19*, 782.
(18) Ruelle, P. *J. Comput. Chem.* **1987**, *8*, 158.
(19) Ruelle, P. *J. Chem. Soc., Perkin Trans. 2* **1986**, *12*, 1953.
(20) Glukhovtsev, M. N.; Bach, R. D.; Laiter, S. *J. Org. Chem*. **1997**, *62*, 4036.
(21) Li, J.; Brill, T. B. *J. Phys. Chem. A* **2002**, *106*, 9491.
(22) Kieke, M. L.; Schoppelrei, J. W.; Brill, T. B. *J. Phys. Chem*. **1996**, *100*, 7455.
(23) Schoppelrei, J. W.; Kieke, M. L.; Wang, X.; Klein. M. T.; Brill, T. B. *J. Phys. Chem*. **1996**, *100*, 14343.
(24) Maiella, P. G.; Schoppelrei, J. W.; Brill, T. B. *Appl. Spectroscopy* **1999**, *53*, 351.
(25) Cvetanovic, R. J.; Singleton, D. L. *Int. J. Chem. Kinetics* **1977**, *9*, 481.
(26) La Marca, C.; Libanati, C.; Klein, M. T.; Cotter, R. J.; Andrews, S. M. *Preprints of Papers, ACS Fuel Div*., **1991**, *36*, 676.
(27) Frisch, M. J.; Trucks, G. W.; Schlegel, H. B.; Scuseria, G. E.; Robb, M. A.; Cheeseman, J. R.; Zakrzewski, V. G.; Montgomery, J. A., Jr.; Stratmann, R. E.; Burant, J. C.; Dapprich, S.; Millam, J. M.; Daniels, A. D.; Kudin, K. N.; Strain, M. C.; Farkas, O.; Tomasi, J.; Barone, V.; Cossi, M.; Cammi, R.; Mennucci, B.; Pomelli, C.; Adamo, C.; Clifford, S.; Ochterski, J.; Petersson, G. A.; Ayala, P. Y.; Cui, Q.; Morokuma, K.; Malick, D. K.; Rabuck, A. D.; Raghavachari, K.; Foresman, J. B.; Cioslowski, J.; Ortiz, J. V.; Stefanov, B. B.; Liu, G.; Liashenko, A.; Piskorz, P.; Komaromi, I.; Gomperts, R.; Martin, R. L.; Fox, D. J.; Keith, T.; Al-Laham, M. A.; Peng, C. Y.; Nanayakkara, A.; Gonzalez, C.; Challacombe, M.; Gill, P. M. W.; Johnson, B. G.; Chen, W.; Wong, M. W.; Andres, J. L.; Head-Gordon, M.; Replogle, E. S.; Pople, J. A. *Gaussian 98*, revision A.9; Gaussian, Inc.: Pittsburgh, PA, 1998.
(28) Becke, A. D. *J. Chem. Phys.* **1993**, *98*, 5648.
(29) Lee, C.; Yang, W.; Parr, R. G. *Phys. Rev. B* **1988**, *37*, 785.
(30) Butler, J. N. *Ion Equilibrium, Solubility and pH Calculation*; John Wiley & Sons: New York, 1998; p 368.
(31) Marshall, W. L.; Franck, E. U. *J. Phys. Chem. Ref. Data* **1981**, *10*, 295.
(32) Uematsu, M.; Franck, E. U. *J. Phys. Chem. Ref. Data* **1980**, *9*, 1291.
(33) Serjeant, E. P.; Dempsey, B. *Ionization Constants of Organic Acids in Aqueous Solutions*; Pergamon: Oxford, 1979.
(34) Lindsay, W. T. *Proc. Int. Water Conf. Eng. Soc. W. Pa*. **1980**, *41*, 284.
(35) Nagy, P. I.; Dunn, W. J. III.; Alagona, G.; Ghio, C. *J. Phys. Chem.* **1993**, *97*, 4628.
(36) Nagy, P. I.; Smith, D. A.; Alagona, G.; Ghio, C. *J. Phys. Chem*. **1994**, *98*, 486.
(37) Shapley, W. A.; Bacskay, G. B.; Warr, G. G. *J. Phys. Chem. B.* **1998**, *102*, 1938.
(38) Tautermann, C.; Voegele, A. F.; Loeting, T.; Kohl, I.; Hallbrucker, A.; Mayer, E.; Liedl, K. *Chem. Eur. J.* **2002**, *8*, 66.
(39) Akiya, N.; Savage, P. E. *AIChE J.* **1998**, *44*, 405.
(40) Zipe, H.; Apaydin, G.; Houk, K. N. *J. Am. Chem. Soc*. **1995**, *117*, 8606.
(41) Gao, J. *J. Am. Chem. Soc*. **1995**, *117*, 8600.
(42) Fredricks, S. Y.; Jordan, K. D.; Zwier, T. S. *J. Phys. Chem.* **1996**, *100*, 7810.
(43) Sicinska, D.; Paneth, P.; Truhlar, D. G. *J. Phys. Chem. B* **2002**, *106*, 2708.